Title
Activation of a cryptic splice site in the mitochondrial elongation factor GFM1 causes combined OXPHOS deficiency

Authors
Simon, Mariella T
Ng, Bobby G
Friederich, Marisa W
et al.

Publication Date
2017-05-01

DOI
10.1016/j.mito.2017.02.004

Peer reviewed

HHS Public Access

Author manuscript

Mitochondrion. Author manuscript; available in PMC 2017 May 25.

Published in final edited form as:

Mitochondrion. 2017 May ; 34: 84–90. doi:10.1016/j.mito.2017.02.004.

Activation of a cryptic splice site in the mitochondrial elongation factor *GFM1* causes combined OXPHOS deficiency☆

Mariella T. Simon[a,b,1], **Bobby G. Ng**[c,1], **Marisa W. Friederich**[d], **Raymond Y. Wang**[a,e], **Monica Boyer**[a], **Martin Kircher**[f], **Renata Collard**[d], **Kati J. Buckingham**[g], **Richard Chang**[a,e], **Jay Shendure**[f,h], **Deborah A. Nickerson**[f], **Michael J. Bamshad**[f,g], **University of Washington Center for Mendelian Genomics**, **Johan L.K. Van Hove**[d], **Hudson H. Freeze**[c], and **Jose E. Abdenur**[a,e,*]

[a]Division of Metabolic Disorders, CHOC Children's, Orange, CA, USA

[b]Department of Developmental and Cell Biology, University of California Irvine, Irvine, CA, USA

[c]Human Genetics Program, Sanford Children's Health Research Center, Sanford-Burnham-Prebys Medical Discovery Institute, La Jolla, CA, USA

[d]Department of Pediatrics, Section of Clinical Genetics and Metabolism, University of Colorado, Aurora, CO, USA

☆**Grant Support:** National Institutes of Health grant (R01DK99551) and the Rocket Fund to HHF. Sequencing was provided by the University of Washington Center for Mendelian Genomics (UW-CMG) and was funded by the National Human Genome Research Institute and the National Heart, Lung and Blood Institute grant 5UM1HG006493 to DAN and MJB. MTS is supported by a grant from the Fry Family Foundation to JEA (40031028). RYW is supported by the Brian and Caris Chan Family Foundation (40021698). The work is supported by Miracles for Mito to M.F. and J.V.H. The energy lab (E-Lab) at CHOC Children's is supported by grants from the Fry family foundation and the PSF Tithe Committee.

*Corresponding author at: Jose E. Abdenur, Division of Metabolic Disorders, CHOC Children's, CHOC West, 1201 West La Veta Ave, Orange, CA 92868, USA. jabdenur@choc.org (J.E. Abdenur).

[1]These authors contributed equally.

Informed consent: All procedures followed were in accordance with the ethical standards of the responsible committee on human experimentation (institutional and national) and with the Helsinki Declaration of 1975, as revised in 2000 (http://www.wma.net/en/30publications/10policies/b3/). Medical record review and photography were performed after the family provided written consent under CHOC Institutional Review Board Protocol #130990.

Animal rights: This article does not contain any studies with animal subjects performed by any of the authors.

Contributions of individual authors

Mariella Simon drafted and edited the manuscript, performed experiments on patient fibroblasts, prepared figures and obtained informed consent.
Bobby G. Ng drafted and edited the manuscript, performed experiments on patient fibroblasts and prepared figures.
Marisa W. Friederich performed experiments on patient fibroblasts and prepared figures.
Raymond Y. Wang provided direct patient care and edited the manuscript providing critical feedback.
Monica Boyer drafted the case report and provided direct patient care.
Martin Kircher carried out exome sequencing and data analysis.
Renata Collard performed experiments on patient fibroblasts and prepared figures.
Kati J. Buckingham carried out exome sequencing and data analysis.
Richard Chang provided direct patient care.
Jay Shendure carried out exome sequencing and data analysis.
Deborah A. Nickerson carried out exome sequencing and data analysis.
Michael J. Bamshad carried out exome sequencing and data analysis.
Johan van Hove: Conceived experiments on patient fibroblasts and edited the manuscript providing critical feedback.
Hudson H. Freeze edited the manuscript providing critical feedback.
Jose E. Abdenur provided direct patient care and edited the manuscript providing critical feedback.

All authors have reviewed the final version of the manuscript.

Conflict of interest

The authors declare that they have no conflict of interest.

[e]Department of Pediatrics, University of California Irvine, Irvine, CA, USA

[f]Department of Genome Sciences, University of Washington, Seattle, WA, USA

[g]Department of Pediatrics, University of Washington, Seattle, WA, USA

[h]Howard Hughes Medical Institute, University of Washington, Seattle, WA, USA

Abstract

We report the clinical, biochemical, and molecular findings in two brothers with encephalopathy and multi-systemic disease. Abnormal transferrin glycoforms were suggestive of a type I congenital disorder of glycosylation (CDG). While exome sequencing was negative for CDG related candidate genes, the testing revealed compound heterozygous mutations in the mitochondrial elongation factor G gene (*GFM1*). One of the mutations had been reported previously while the second, novel variant was found deep in intron 6, activating a cryptic splice site. Functional studies demonstrated decreased GFM1 protein levels, suggested disrupted assembly of mitochondrial complexes III and V and decreased activities of mitochondrial complexes I and IV, all indicating combined OXPHOS deficiency.

Keywords

GFM1; Mitochondrial disease; Congenital disorders of glycosylation; Mitochondrial elongation factor; Cryptic splice site

1. Introduction

Mitochondria are the hub of cellular metabolism, respiration, energy production as well as sites of reactive oxidative species (ROS), heme and steroid generation. Furthermore they buffer cellular calcium flux, regulate redox states, control cell cycle and cell death. The mitochondrial network is the only cellular organelle of the animal kingdom carrying its own dedicated DNA (mtDNA), which in humans codes for thirteen essential mitochondrial proteins (Wallace, 2013). Their translation requires a dedicated protein synthesis machinery, independent from its cytoplasmic counterpart (Smits et al., 2010a). Approximately 1500 nuclear genes have been attributed to mitochondrial biogenesis and metabolism (Pagliarini et al., 2008), of which about 10% are thought to play a role in mitochondrial translation (Rotig, 2011). Since mitochondria retain a dedicated mitochondrial protein synthesis machinery to synthesize mtDNA encoded proteins, mutations in mitochondrial elongation factor genes cause mitochondrial translational defects. Three mitochondrial elongation factors have been described to date: EF-Tu (*TUFM*; MIM#602389), EF-Ts (*TSFM*; MIM#604723), and EF-G1 (*GFM1*; MIM#606639). The mitochondrial elongation factor EF-Tu delivers cognate amino-acylated mitochondrial tRNAs to the ribosomal binding site in a GTP-dependent manner. Once the amino acid has been delivered, GDP bound EF-Tu is released and subsequently recharged with GTP via the elongation factor Ts (EF-Ts). EF-G1, also a GTPase, enforces the elongation-dependent movement of mtDNA encoded tRNAs through the mitochondrial ribosomes by removing the de-acetylated tRNA and replacing it with the peptidyl-tRNA (Christian and Spremulli, 2012). Mitochondria generate ATP via oxidative

phosphorylation (OXPHOS), a process which depends on the concerted action of five mitochondrial protein complexes (complex I through V). Complexes I, III, IV and V all contain at least one mtDNA encoded subunit, while complex II is encoded completely by nuclear DNA (Wallace, 2013). A defect in any of the elongation factors is therefore predicted to result in abnormalities of multiple OXPHOS related complexes, a type of mitochondrial dysfunction since termed “combined oxidative phosphorylation deficiency”, or COXPD (COXPD4 (MIM#610678) for *TUFM*, COXPD3 (MIM#610505) for *TSFM* and COXPD1 (MIM#609060) for *GFM1*). Mutations in all three mitochondrial elongation factors have been associated with severe mitochondrial disease phenotypes (Boczonadi and Horvath, 2014).

Herein we describe clinical, laboratory and molecular findings for two brothers with mutations in *GFM1*. We highlight the survival and stable clinical course in one of the siblings at seven years of age and the unusual findings of repeated transferrin glycoforms suggesting a type I congenital disorder of glycosylation (CDG). We therefore propose to consider mitochondrial disease in the differential diagnosis following abnormal transferrin testing. We also describe a novel, intronic *GFM1* mutation, which results in the predominant use of a non-canonical *GFM1* isoform and secondary GFM1 protein instability. Our findings demonstrate the importance of choosing exome capture kits and data annotation, which not only cover the canonical isoform of a gene but all potential transcripts (Chilamakuri et al., 2014).

2. Materials and methods

2.1. Exome sequencing

One microgram (μg) of genomic DNA was subjected to a series of shotgun library construction steps, including fragmentation through acoustic sonication (Covaris), end-polishing (NEBNext End Repair kit), A-tailing (NEBNext dA Tailing kit), and ligation of 8 base pairs (bp) barcoded sequencing adaptors (Enzymatics Ultrapure T4 Ligase). Libraries were automatically size selected for fragments 350–550 bp in length with the automated PippinPrep cartridge system. Prior to sequencing, the library was amplified via PCR (BioRad iProof).

1 μg of barcoded shotgun library was hybridized to capture probes targeting 64 mega bases (Mb) of coding exons and microRNA (miRNA) (Roche Nimblegen SeqCap EZ Human Exome Library v3.0) with custom blockers complimentary to the full length of the flanking adaptor and barcodes. Enriched libraries were amplified via PCR before sequencing (BioRad iProof). Library quality was determined by examining molecular weight distribution and sample concentration (Agilent Bioanalyzer). Pooled, barcoded libraries were sequenced via paired-end 50 bp reads with an 8 bp barcode read on Illumina HiSeq sequencers.

De-multiplexed BAM files were aligned to the human reference (hg19) using the Burrows-Wheeler Aligner. Read data from a flow-cell lane were treated independently for alignment and QC purposes in instances where the merging of data from multiple lanes was required. All aligned read data were subjected to: (1) Removal of duplicate reads (Picard), (2) indel realignment using the GATK IndelRealigner and (3) base qualities recalibration using GATK

TableRecalibration. Variant detection and genotyping were performed using the UnifiedGenotyper (UG) tool from GATK. Variant data for each sample were formatted (variant call format [VCF]) as "raw" calls that contained individual genotype data for one (GATK 1.0) or multiple samples (GATK 1.6–11), and flagged using the filtration walker (GATK) to mark sites that were of lower quality and potential false positives (e.g. quality scores (≤50), allelic imbalance (≥0.75), long homopolymer runs (>3), and/or low quality by depth (QD<5)).

The single sample VCF files were filtered for 1000 Genomes and NHLBI GO Exome Sequencing Project variants with a frequency of >5% cutoff, a minimum quality value (QUAL) of 30, and a minimum coverage (DP) of 8. All remaining variants were further filtered for the overlap with segmental duplications (UCSC genomicSuperDups) and were required a mapability of 1 (UCSC wgEncodeDukeMapabilityUniqueness20bp). Variants were annotated using the Ensembl Variant Effect Predictor.

2.2. Cell culture

Primary human skin fibroblasts were established from 3 mm punch biopsy. Tissue was grown on plates coated with fibronectin (10 μg/mL of PBS) (LifeTechnologies) in alpha MEM with 1× nonessential aminoacids (NEAA) (LifeTechnologies), Primocin (Invivogen) and 15% FBS (Hyclone-Fetal Clone 3). Established cultures were maintained in DMEM, 1× NEAA, 1× Antibiotic/Antimycotic (all LifeTechnologies) and 15% FBS (Hyclone-Fetal Clone 3) at 37 °C in 5% CO_2.

2.3. Immunoblotting

Cells were lysed on ice in RIPA Buffer (Pierce) supplemented with Protease inhibitor cocktail (50ul/mL) (Sigma) for 30 min at 4 °C and cleared at 16,000 rpm for 20 min. Protein concentration was determined in triplicate via DC protein assay (Biorad). Lysates were stored in Nupage LSD sample buffer (LifeTechnologies) at −20 °C. SDS PAGE was performed using NuPage Bis-Tris Gels and NuPage MOPS running buffer (LifeTechnologies). Proteins were blotted onto PVDF membrane (LifeTechnologies) and blocked for 30 min at room temperature (RT) with Fast Blocking buffer (Pierce). Membranes were incubated with 1:1000 anti-GFM1 (Abcam, ab176786 as well as ab171945) and 1:100,000 anti-beta Actin (Abcam, ab8227) or total OXPHOS human WB antibody cocktail (Abcam, ab110411) at 4 °C overnight, washed briefly with 1× TBS-T and incubated with HRP-conjugated goat anti-rabbit (Abcam, ab6721) or HRP-conjugated goat anti-mouse IgG (Abcam, ab97023) at RT for 1 h. Membranes were then washed 3× with 1× TBS-T at RT for 5 min each and proteins were detected with SuperSignal Chemi-luminescent substrate (LifeTechnologies) and imaged on CL-Xposure film (LifeTechnologies).

2.4. BN-PAGE with in-gel activity staining assay

Mitochondria were isolated from cultured fibroblasts following the protocol of van Coster et al. (2001). Following solubilization of the mitochondria, the isolated OXPHOS membrane protein complexes were analyzed by blue native polyacrylamide gel electrophoresis (BN-PAGE) with in-gel activity stain as described (Smet et al., 2006; van Coster et al., 2001;

Chatfield et al., 2015). This assay allows for both the evaluation of the activity and assembly of the OXPHOS complexes. For example, the presence of additional bands of lower molecular weight of complex V, due to incomplete assembly can be observed in defects of complex V assembly as well as defects in mitochondrial transcription or translation (Smet et al., 2009).

3. Results

3.1. Case report patient 1

Patient 1 (P1) was born after a pregnancy complicated by early 1st trimester bleeding at 37 weeks gestation with normal birth weight and uncomplicated postnatal course. At 3 months of age he was hospitalized due to a respiratory syncytial virus (RSV) infection. Developmental delay, microcephaly, hypertonicity, and visual inattention were noticed and he was referred to our center for evaluation. Family history was significant for an affected, deceased male sibling [patient 2 (P2)], who was born 4 years prior to P1 (Fig. 1A). Evaluation of P1 was positive for multiple dysmorphic features (Fig. 1B). Ophthalmological exam, MRI of the brain, and echocardiogram performed at 5 months of age were normal.

Initial biochemical evaluations were significant for abnormal carbohydrate deficient transferrin (CDT) testing performed by affinity chromatography, mass spectrometry (Mayo Clinic) (high mono:di-oligo ratio of 0.176; reference range <0.100, with normal a-oligo:di-oligo ratio of 0.019; reference range <0.050, persistent lactic acidemia (2.4–11.1 mmol/L; reference range <2.2) and increased alanine (595 μmol/L; reference range 143–439). Other routine metabolic screening labs were unremarkable, including normal ammonia, acylcarnitine profile, homocysteine, urine organic acids, urine guanidinoacetate, and 7-dehydrocholesterol level. Repeat CDT testing with the same methodology demonstrated similar abnormalities. A third sample, analyzed by MALDI-TOF (Emory Genetics Laboratory), appeared consistent with a type I glycosylation defect.

By 4.5 months of age P1 developed seizures, characterized as infantile spasms, and was started on antiepileptic medication (topiramate). At 6 months of age he had a right inguinal hernia repair and percutaneous endoscopic gastrostomy tube placement, secondary to persistent dysphagia and recurrent emesis. At 7 months of age, renal tubular acidosis was suspected based on persistent non-anion gap metabolic acidosis with simultaneous urine pH>7.0. Treatment with citric acid/sodium citrate (Bicitra®) at 3 mEq/kg/day was initiated. Hepatomegaly and persistent mild elevation of transaminases with normal bilirubin and coagulation factors were noted at 8 months of age with intermittent low albumin levels. During his frequent hospitalizations due to intercurrent illnesses associated with emesis, it was found that his lactic acidosis improved markedly with high glucose infusion rates exceeding 8 mg/kg/min. At 2 years of age frequent nose bleeds were suggestive of coagulopathy and he was found to have type 1 von Willebrand disease with a ristocetin level of 39. His bleeding symptoms have been stable with monthly human von Willebrand factor complex infusions and aminocaproic acid. Due to his family history, cardiovascular status was closely monitored and at 4.5 years of age an echocardiogram revealed borderline left ventricular hypertrophy with normal left ventricular function. However, follow up echocardiograms showed resolution of his ventricular enlargement without any specific

treatment. Over time, the clinical condition for P1 has improved, with reduced frequency, severity, and duration of hospitalizations and improved tolerance to gastrostomy tube feedings. He has remained seizure free on treatment with topiramate. Liver synthetic function is borderline abnormal (albumin 3.7 mg/dL; reference range >3.8, international normalized ratio 1.08–1.18; reference range <1.15, partial thromboplastin time 36.6–41.9 s; reference range <38 s) with persistently borderline elevated transaminases (AST 43–102 units/L; reference range b46 units/L; ALT 34–94 units/L; reference range <35 units/L) and mild hepatomegaly. At 7 years of age, his vision and hearing appear intact and he continues to make small developmental gains, is interactive, able to say simple words and sit unassisted.

3.2. Case report patient 2

At birth, patient 2 (P2) was found to have symmetric intrauterine growth retardation (IUGR), cleft palate, and hypospadias. He developed metopic forehead ridging, laryngomalacia, concentric left ventricular hypertrophy, transient hepatomegaly, bilateral renal pyelectasis and spasticity. Severe feeding intolerance eventually required placement of a jejunostomy tube. Biochemical testing was unrevealing, except for persistent lactic acidosis and an acylcarnitine profile with elevated C4OH, which was interpreted as consistent with ketosis. A defect in pyruvate carboxylase was suspected, but enzyme activity in fibroblasts was normal. P2 had multiple hospitalizations, with the last one taking place at 8 months of age that eventually progressed to multi-organ failure and death at 10 months of age. At the time no specific diagnosis was established for P2.

Medical record review and photography were performed after family provided consent under CHOC Institutional Review Board Protocol #130990. Due to the abnormal ESI-MS/MS CDT testing and unusual clinical and biochemical phenotype of P1, whole exome sequencing (WES) was performed by the University of Washington Center for Mendelian Genomics (Bamshad et al., 2011). No candidate variants were identified in known or putative CDG genes. The analysis did however demonstrate a previously reported mutation in *GFM1* (ENST00000486715), at position c.748C>T, p.Arg250Trp (Smits et al., 2010b). The mother of both patients was found to be a carrier of the mutation. This finding prompted additional analyses of sequencing data, which revealed a second, intronic variant in *GFM1*, inherited from the father at position c.689+908 G>A, p.Gly230_231Glnins19 (ENST00000486715). The two sequence variants segregated with the disease since P2 was found to also be compound heterozygous for both mutations, and the healthy sister bore neither mutation (Fig. 1A, Section 3.1). For cDNA numbering, the use of +1 represents the A of the ATG translation initiation codon in the canonical GFM1 transcript ENST00000486715. All variants have been deposited in the LOVD3.0 (http://databases.lovd.nl/).

3.3. c.689+908 G>A induces the activation of a cryptic splice site

The effect of the intronic variant at position c.689+908 G>A on mRNA splicing was assessed. Isoform 1 of *GFM1* (GFM1-001 ENST00000486715) is comprised of 18 exons which code for a protein of 751 amino acids (UniProtKB: Q96RP9), while the noncanonical isoform 2 (GFM1-004 ENST00000264263) includes an additional exon between exons 5

and 6 (exon 5b) of GFM1-001 and codes for a protein of 770 amino acids (UniProtKB - Q96RP9). The intronic variant observed in both affected males hypothetically affects the splice donor of exon 6 of the noncanonical GFM1-004 at position c.746+4 G>A (Fig. 1C, Section 3.1). The human splice finder software predicts a significant increase in the strength of the splice donor GT of GFM1-004 intron 6/7 from 88.33 to 97.67 (Desmet et al., 2009). To investigate the variant's effect on *GFM1* mRNA splicing in our patients, we reverse transcribed RNA isolated from the fibroblasts of P1 and P2 and amplified the exon/intron junction of GFM1-001 exons 5 and 6 via reverse transcriptase polymerase chain reaction. These experiments revealed an amplicon not observed in two independent controls of increased size (Fig. 2A, Section 3.3).

3.4. Sequencing analysis of amplified cDNA reveals an in-frame insertion

Sequencing analysis of the isolated band revealed an addition of 57 nucleotides, which are identical to exon 6 of GFM1-004 (Fig. 1C, Section 3.1). We therefore conclude that in primary fibroblasts the *GFM1* variant c.689+908 G>A (p.Gly230_231Glnins19) induces the expression of the noncanonical isoform GFM1-004 rather than canonical GFM1-001 from this allele, which extends the G' domain of EFG1 by 19 amino acids.

3.5. Blue native polyacrylamide gel electrophoresis with in-gel activity stain reveals a mitochondrial complex V assembly defect and decreased activity for complexes I and IV

Due to the molecular findings in *GFM1*, functional analyses to assess the activity and integrity of the mitochondrial respiratory chain complexes were performed for both patients. Using blue native polyacrylamide gel electrophoresis (BN-PAGE) with in-gel activity stain of mitochondrial lysates from cultured fibroblasts showed P2 had decreased activity for mitochondrial complex I and IV; while P1 showed decreased activity for complex IV but normal activity for complex I (Fig. 2B, Section 3.3). Both patients showed the clear presence of pathognomonic additional lower molecular weight bands of mitochondrial complex V on blue native PAGE analysis, indicative of incomplete assembly or reduced stability of the holocomplex V, a finding consistent with defects of complex V assembly as well as defects in mtDNA maintenance, transcription or translation (Fig. 2B, Section 3.3) (van Coster et al., 2001; Smet et al., 2006; Smet et al., 2009).

3.6. Western blot for GFM1 shows decreased protein levels

Immunoblotting revealed significantly decreased GFM1 protein levels for cell lysates from both patients employing an anti-GFM1 antibody (Abcam, ab176786) with known immunogen location corresponding to aa581–742 (Q96RP9) (data not shown) as well as an anti-GFM1 antibody (Abcam, ab171945) with proprietary immunogen location (Fig. 2C, Section 3.3). Anti-beta actin (Abcam) was used to show equal loading. This further supports our findings that the mutations have functional consequence.

3.7. Western blot for OXPHOS subunits shows decreased protein levels for complexes III and IV

Immunoblotting with an OXPHOS antibody cocktail (Abcam, ab110411) on whole cell lysates from P1 and P2 showed decreased protein levels of the nuclear encoded complex III

subunit ubiquinol-cytochrome *c* reductase core protein II (UQCRC2) as well as of the mtDNA encoded complex IV subunit cytochrome *c* oxidase subunit 2 (COXII) in both patients as compared to control (Fig. 2D, Section 3.3). Since mitochondrial complex II has no mtDNA encoded subunits the anti-succinate dehydrogenase complex subunit b antibody (SDHB) was used as a loading control. We also re-probed the membrane with an anti-beta-Actin antibody raised against a different species than the OXPHOS antibody cocktail as an additional loading control. The findings suggest dysfunction of the assembly of complex III, which has been shown to be associated with decreased levels of UQCRC2, a core protein of complex III (Miyake et al., 2013). Decreased levels of COXII further support a translational defect in patient cell lines affecting mtDNA encoded proteins and are consistent with results shown for BNG analysis.

4. Discussion

In 2004, Coenen et al. reported the first patient with *GFM1* mutations (Coenen et al., 2004). Since then, a total of 15 patients in 12 families have been published (Supp. Table S1). Prevalent features in these patients include early onset (sometimes neonatal) encephalopathy, liver disease, feeding difficulties, failure to thrive, and lactic acidosis. Liver failure was present in 7 of 13 patients; all of them deceased at <2 months of age. IUGR, microcephaly, and minor dysmorphic features have also frequently been described. Notably, cardiomyopathy and renal tubular defects, which are relatively common manifestations of mitochondrial diseases, have not been reported in these patients. This has been attributed to tissue specific differences in stability of GFM1 mutant protein as well as expression levels of the mitochondrial translation factors (Antonicka et al., 2006). Similar to the previously described cases our patient also had early onset of disease, showed dysmorphic features, mild liver involvement and persistent lactic acidemia. P2 had left ventricular hypertrophy but overt cardiomyopathy did not develop in P1. The finding of a pathogenic *GFM1* mutation together with the phenotype of our patients therefore provided enough evidence to warrant additional studies into this gene.

The previously reported missense variant at position c.748C>T (p.Arg250Trp) was found to be homozygous in a patient with mitochondrial encephalopathy (Smits et al., 2010b). The girl, who died at 2 years of age, developed seizures at 2 months old while seizures did not start until 4.5 months of age in P1. Like our patient she was hypotonic, had feeding problems, nystagmus and was borderline microcephalic but unlike our patient was not dysmorphic. Her MRI was abnormal for a small frontal cortex, delayed myelination and thinning of the corpus callosum, while P1 discussed in this report had normal MRI at 5 months of age. Similar to our patients her lactate levels were consistently elevated however, in contrast to our case and other reported patients, her liver function tests were repeatedly normal. Functional mitochondrial tests for the girl revealed normal oxidative phosphorylation levels in muscle homogenate, while the same test in fibroblasts showed severely decreased activity of mitochondrial complex I and complex IV and moderate decrease for mitochondrial complex III. This is consistent with mitochondrial analyses on fibroblasts for our patients via blue native polyacrylamide gel electrophoresis (BN-PAGE) with in-gel activity stain, which demonstrated decreased activity for mitochondrial complex I and IV for P2 but only a decrease in complex IV for P1 (Fig. 2B, Section 3.3). To find

mitochondrial complex I affected to a lesser degree than mitochondrial complex IV is puzzling, since mitochondrial complex I has the highest number of mtDNA encoded subunits. However, similar findings have been reported in other *GFM1* related publications but cannot currently be explained (Coenen et al., 2004). Cells from P1 and P2 also showed pathognomonic subcomplexes of complex V, likely reflecting either incomplete assembly or decreased stability, and typically seen in defects of mtDNA maintenance, transcription or translation defect via blue native gel electrophoresis (Smet et al., 2009; Wittig et al., 1797; Carrozzo et al., 2006). The amount of the alpha-subunit on the western blot was normal reflecting the normal amounts of the F_1 subcomplex, which does not require the presence of mitochondrial DNA encoded subunits, and hence is not sensitive to mitochondrial translation defects (Fig. 2B and D, Section 3.3). As described previously for the female patient with the homozygous p.Arg250Trp mutations, western blotting of cell lysates from our patients also revealed decreased levels of GFM1 protein (Fig. 2C, Section 3.3). Although we cannot exclude the possibility that the anti-GFM1 used in our experiment may have been unable to detect a hypothetical GFM1 protein with a 19 amino acid insertion, we do not have evidence for such a protein species at this time (Fig. 2C, Section 3.3). To further address this issue, the protein lysates were interrogated with two different anti-GFM1 antibodies and both antibodies indicated significantly reduced GFM1 protein levels. Western blotting employing an OXPHOS antibody cocktail furthermore supports abnormal GFM1 function leading to combined OXPHOS deficiency with decreased levels of COXII and UQCRC2 (Fig. 2D, Section 3.3).

Prognosis for patients with *GFM1* mutations is strikingly poor, as all patients died in infancy, with the exception of one milder case reported to be alive at 6 years of age (Brito et al., 2015). This patient's mild case could not be explained by mutation type since she is compound heterozygous for one nonsense and a previously reported severe missense mutation. The authors emphasize that their patient shares many features with other *GFM1* cases with early onset failure to thrive, encephalopathy and seizures stating at 7 months of age as well as persistent lactic acidosis with a maximum of 4.87 mmol/L but lacks liver involvement. Our report now adds a second patient with long-term survival and stable clinical course at age 7 years. In contrast his older brother died at 10 months of age from multiple organ failure. Since the difference in severity for the brothers described here cannot be explained by mutation location in *GFM1* we speculate that it is due to differences in modifier genes, exposure to infections at a vulnerable age or levels of care.

The finding for P1 of intermittent abnormal glycosylation may shed additional light on an underlying cause for variability in disease severity and expression. Mitochondrial diseases share with CDGs the challenge that both are extremely difficult to diagnose due to their multi-systemic involvement, as well as extensive clinical and locus heterogeneity (Freeze et al., 2015). In fact, CDG patients are very likely to be underdiagnosed or even misdiagnosed as mitochondrial disease (Helander, 2004). We present a kindred with multisystemic, infantile onset disease who initially was thought to have a type I CDG due to abnormal transferrin glycoforms. Abnormal protein glycosylation is not a common finding associated with mitochondrial disease, although CDT testing may not be routinely performed in patients suspected of having mitochondrial disorders. Only one of the currently published reports on *GFM1* describes testing for CDG, which were found to be normal in an infant

with progressive hepatoencephalopathy at 4 months of age (Balasubramaniam et al., 2012). In contrast, our patient did not show abnormal liver functions until 8 months of age, three months after the first abnormal CDT test was obtained. Our findings follow the report of another patient initially diagnosed with a CDG, but eventually found to have mutations in the mitochondrial DNA helicase Twinkle (Bouchereau et al., 2016). Pregnancy history for this patient was significant for a maternal dengue virus infection during the first trimester. The patient developed vomiting in the first weeks of life and by 5 months hypotonia and psychomotor regression were noted. This patient had repeated abnormal glycosylation profiles, which were suggestive of a type I CDG. It is interesting that our patient as well as the patient reported by Bouchereau both showed defects in N-glycosylation. Bio-synthesis and processing of N-glycans occurs in the endoplasmic reticulum (ER) and is continued in the Golgi. It has long been known that the ER and mitochondria share important membrane contact sites termed “MAM” (Mitochondrial Associated ER Membranes), which are heavily involved in calcium exchange and signaling (Rizzuto et al., 1998). ER calcium levels control the manufacture of many important secretory enzymes including those involved in N-glycosylation (Michalak et al., 2002). Disruption of MAM integrity has recently been shown as a frequent finding of neurodegenerative disease development (Scorrano, 2008; Raturi and Simmen, 2013; Stoica et al., 2014). MAM also plays an important role in the immune defense response to RNA viruses since the Mitochondrial Anti-Viral Signaling co-factor MAVS is located at MAM (Horner et al., 2011). MAVS forms prion like aggregates on the outer mitochondrial membrane in response to RNA virus infections (Hou et al., 2011). It may therefore be speculated that remodeling of MAM during intermittent illnesses may affect glycosylation. While the possibility cannot be ruled out that WES sequencing, performed for this as well as the patient reported by Bouchereau, missed a mutation in a CDG gene it suggests that some mitochondrial diseases may manifest with disruption of glycosylation. In fact, perhaps abnormal markers of N-glycosylation should result in additional molecular and biochemical evaluations for mitochondrial electron transport chain defects. Our findings also reinforce the limitations of exome sequencing technologies and should bring awareness of such to the clinicians interpreting patient reports. The ExAc database is an aggregate data set of 60,706 human exome sequences. Therefore variant frequency information for exons of canonical transcripts is on average comprised of 120,000 alleles. The low Ex-Ac coverage of only 12,324 alleles for the c.689+908 GNA mutation demonstrates that most exome capture methods do not include (or cover) this region of *GFM1*.

5. Conclusion

Our report adds new information to the mutational spectrum of *GFM1* and highlights abnormal N-glycosylation as a potential biochemical marker. We expand the phenotype to include long-term survival in now two cases in this hepatocerebral mitochondrial disorder. Our findings also suggest that patients with *GFM1* mutations are most vulnerable at an early age and then recover and can be relatively stable, a clinical course that has been observed previously in other mitochondrial protein synthesis defects (Boczonadi et al., 2015). Early detection of the disease based on modern sequencing technologies may therefore lead to

improved supportive treatment, slowing decline in health and reducing severity of symptomatology.

Supplementary Material

Refer to Web version on PubMed Central for supplementary material.

Acknowledgments

We thank the family for providing samples and consenting to this study.

Appendix A. Supplementary data

Supplementary data to this article can be found online at http://dx.doi.org/10.1016/j.mito.2017.02.004.

References

Antonicka H, Sasarman F, Kennaway NG, Shoubridge EA. The molecular basis for tissue specificity of the oxidative phosphorylation deficiencies in patients with mutations in the mitochondrial translation factor EFG1. Hum Mol Genet. 2006; 15(11):1835–1846. [PubMed: 16632485]

Balasubramaniam S, Choy YS, Talib A, Norsiah MD, van den Heuvel LP, et al. Infantile progressive hepatoencephalomyopathy with combined OXPHOS deficiency due to mutations in the mitochondrial translation elongation factor gene GFM1. JIMD Rep. 2012; 5:113–122. [PubMed: 23430926]

Bamshad MJ, Ng SB, Bigham AW, Tabor HK, Emond MJ, et al. Exome sequencing as a tool for Mendelian disease gene discovery. Nat Rev Genet. 2011; 12(11):745–755. [PubMed: 21946919]

Boczonadi V, Horvath R. Mitochondria. Impaired mitochondrial translation in human disease. Int J Biochem Cell Biol. 2014; 48:77–84. [PubMed: 24412566]

Boczonadi V, Bansagi B, Horvath R. Reversible infantile mitochondrial diseases. J Inherit Metab Dis. 2015; 38(3):427–435. [PubMed: 25407320]

Bouchereau J, Barrot SV, Dupre T, Moore SE, Cardas R, et al. Abnormal glycosylation profile and high alpha-fetoprotein in a patient with twinkle variants. JIMD Rep. 2016

Brito S, Thompson K, Campistol J, Colomer J, Hardy SA, et al. Long-term survival in a child with severe encephalopathy, multiple respiratory chain deficiency and GFM1 mutations. Front Genet. 2015; 6:457.

Carrozzo R, Wittig I, Santorelli FM, Bertini E, et al. Subcomplexes of human ATP synthase mark mitochondrial biosynthesis disorders. Ann Neurol. 2006; 59:265–275. [PubMed: 16365880]

Chatfield KC, Coughlin CR, Friederich MW, Gallagher RC, Hesselberth JR, et al. Mitochondrial energy failure in HSD10 disease is due to defective mtDNA transcript processing. Mitochondrion. 2015; 21:1–10. [PubMed: 25575635]

Chilamakuri CSR, Lorenz S, Madoui MA, Vodak D, Sun J, et al. Performance comparison of four exome capture systems for deep sequencing. BMC Genomics. 2014; 15:449. [PubMed: 24912484]

Christian BE, Spremulli LL. Mechanism of protein biosynthesis in mammalian mitochondria. Biochim Biophys Acta, Gene Regul Mech. 2012; 1819(9–10):1035–1054.

Coenen MJ, Antonicka H, Ugalde C, Sasarman F, Rossi R, et al. Mutant mitochondrial elongation factor G1 and combined oxidative phosphorylation deficiency. N Engl J Med. 2004; 351(20): 2080–2086. [PubMed: 15537906]

Desmet FO, Hamroun D, Lalande M, Collod-Beroud G, Claustres M, et al. Human splicing finder. An online bioinformatics tool to predict splicing signals. Nucleic Acids Res. 2009; 37(9):e67. [PubMed: 19339519]

Freeze HH, Eklund EA, Ng BG, Patterson MC. Neurological aspects of human glycosylation disorders. Annu Rev Neurosci. 2015; 38:105–125. [PubMed: 25840006]

Helander A. Testing for congenital disorders of glycosylation by HPLC measurement of serum transferrin glycoforms. Clin Chem. 2004; 50(5):954–958. [PubMed: 15105360]

Horner SM, Liu HM, Park HS, Briley J, Gale M. Mitochondrial-associated endoplasmic reticulum membranes (MAM) form innate immune synapses and are targeted by hepatitis C virus. Proc Natl Acad Sci U S A. 2011; 108(35):14590–14595. [PubMed: 21844353]

Hou F, Sun L, Zheng H, Skaug B, Jiang QX, et al. MAVS forms functional prion-like aggregates to activate and propagate antiviral innate immune response. Cell. 2011; 146(3):448–461. [PubMed: 21782231]

Michalak M, Robert PJM, Opas M. Ca^{2+} signaling and calcium binding chaperones of the endoplasmic reticulum. Cell Calcium. 2002; 32(5–6):269–278. [PubMed: 12543089]

Miyake N, Yano S, Sakai C, Hatakeyama H, Matsushima Y, et al. Mitochondrial complex III deficiency caused by a homozygous UQCRC2 mutation presenting with neonatal-onset recurrent metabolic decompensation. Hum Mutat. 2013; 34(3):446–452. [PubMed: 23281071]

Pagliarini DJ, Calvo SE, Chang B, Sheth SA, Vafai SB, et al. A mitochondrial protein compendium elucidates complex I disease biology. Cell. 2008; 134(1):112–123. [PubMed: 18614015]

Raturi A, Simmen T. Where the endoplasmic reticulum and the mitochondrion tie the knot: the mitochondria-associated membrane (MAM). Biochim Biophys Acta. 2013; 1833(1):213–224. [PubMed: 22575682]

Rizzuto R, Pinton P, Carrington W, Fay FS, Fogarty KE, et al. Close contacts with the endoplasmic reticulum as determinants of mitochondrial Ca^{2+} responses. Science (New York, NY). 1998; 280(5370):1763–1766.

Rotig A. Human diseases with impaired mitochondrial protein synthesis. Biochim Biophys Acta. 2011; 1807(9):1198–1205. [PubMed: 21708121]

de Brito OM, Scorrano L. Mitofusin 2 tethers endoplasmic reticulum to mitochondria. Nature. 2008; 456(7222):605–610. [PubMed: 19052620]

Smet, J., Devreese, B., Beeumen, J., Vancoster, R. Nondenaturing polyacrylamide gel electrophoresis as a method for studying protein interactions: applications in the analysis of mitochondrial oxidative phosphorylation complexes. In: Celis, JE., editor. Cell biology A laboratory handbook. Elsevier Academic Press; Burlington, Massachusetts: 2006. p. 259-264.

Smet J, Seneca S, de Paepe B, Meulemans A, Verhelst H, et al. Subcomplexes of mitochondrial complex V reveal mutations in mitochondrial DNA. Electrophoresis. 2009; 30(20):3565–3572. [PubMed: 19862739]

Smits P, Smeitink J, van den Heuvel Lambert. Mitochondrial translation and beyond: processes implicated in combined oxidative phosphorylation deficiencies. J Biomed Biotechnol. 2010a; 2010(2):1–24.

Smits P, Antonicka H, van Hasselt Peter M, Weraarpachai W, Haller W, et al. Mutation in subdomain G′ of mitochondrial elongation factor G1 is associated with combined OXPHOS deficiency in fibroblasts but not in muscle. Eur J Hum Genet. 2010b; 19(3):275–279. [PubMed: 21119709]

Stoica R, de Vos KJ, Paillusson S, Mueller S, Sancho RM, et al. ER–mitochondria associations are regulated by the VAPB–PTPIP51 interaction and are disrupted by ALS/FTD-associated TDP-43. Nat Commun. 2014

van Coster R, Smet J, George E, de Meirleir L, Seneca S, et al. Blue native poly-acrylamide gel electrophoresis: a powerful tool in diagnosis of oxidative phosphorylation defects. Pediatr Res. 2001; 50(5):658–665. [PubMed: 11641463]

Wallace DC. A mitochondrial bioenergetic etiology of disease. J Clin Invest. 2013; 123(4):1405–1412. [PubMed: 23543062]

Wittig I, Meyer B, Heide H, Steger M, Bleier L, et al. Assembly and oligomerization of human ATP synthase lacking mitochondrial subunits a and A6L. Biochim Biophys Acta. 1797; 2010:1004–1011.

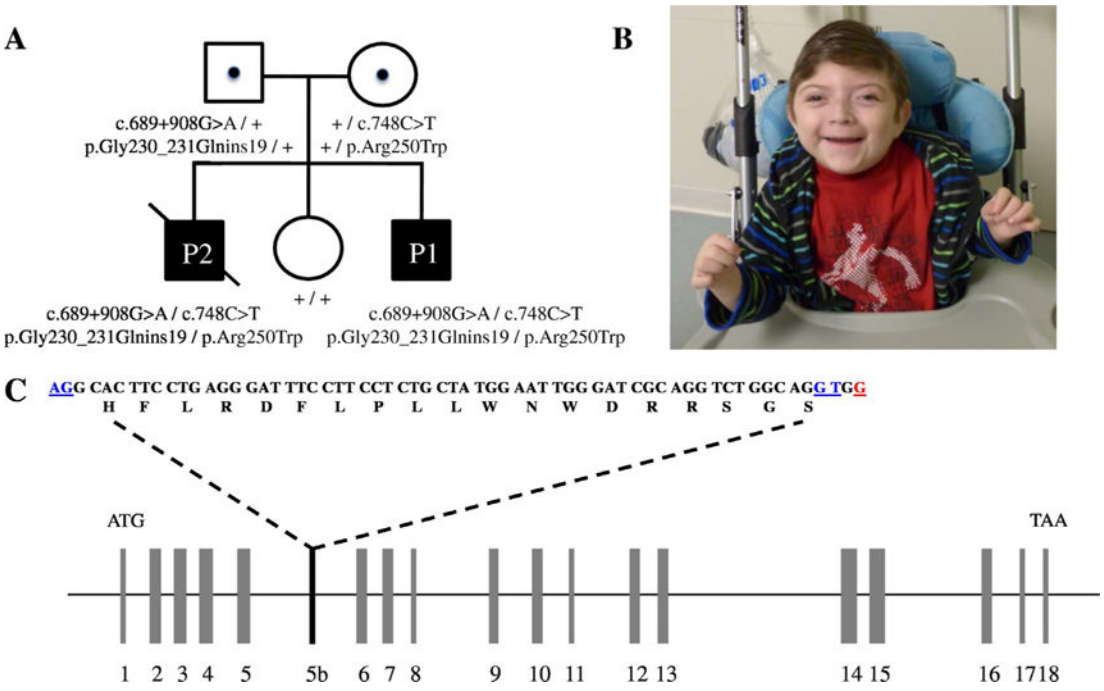

Fig. 1.

Pedigree, clinical photograph and alternative splicing of *GFM1*. A. Pedigree shows segregation of mutations in the family. B. Dysmorphic features include microcephaly, bi-temporal narrowing, metopic ridging, sloping forehead, supraorbital hypoplasia, wide nasal bridge with short nose, short columella, up-turned nasal tip, anteverted nares, long philtrum, mild retrognathia. C. The c.689+908 G>A GFM-001 mutation (depicted in red) leads to the inclusion of 19 amino acids resulting in the preferential expression of GFM-004. The splice donor and acceptor sites of the cryptic exon 5b are depicted in blue. (For interpretation of the references to color in this figure legend, the reader is referred to the web version of this article.)

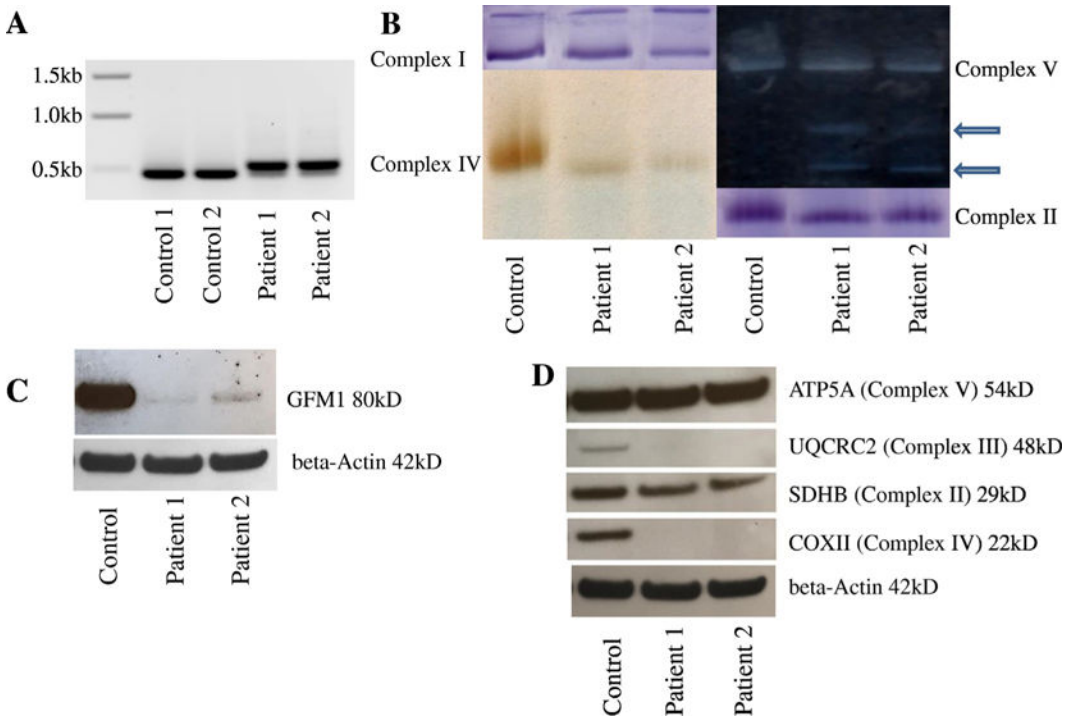

Fig. 2.

Functional analyses in patient fibroblasts. A. mRNA analysis for *GFM1*: Using a forward primer in exon 5 and a reverse primer in exon 6 of GFM1-001 shows increased band size as compared to controls. Sanger Sequencing of the band reveals an “in-frame” insertion of 19 amino acids amplifying GFM1-004. The shorter band is significantly decreased in the patients. B. Blue native polyacrylamide gel electrophoresis (BN-PAGE) with in gel activity staining: left panel: in gel staining for mitochondrial complexes reveal decreased levels of complexes I and IV for patient 2 and complex IV for patient 1. Right panel: activity staining of complex II, which does not have any mtDNA encoded subunits, serves as a loading control. Right Panel: BNG for complex V shows additional, lower molecular weight bands (arrows) indicating incomplete assembly and reduced stability of the complex. C. Immunoblotting: Levels of GFM1 protein are decreased in fibroblast lysates from both patients. D. Immunoblotting: Levels of UQCRC2 and COXII are decreased in fibroblast lysates from patient 1 and 2 while levels of ATP5A are normal. SDHB and beta-Actin are used as loading controls.